Inverse Problems and MRAI
Mapping the Pulse Wave Velocity

Simon Hubmer, Andreas Neubauer, Ronny Ramlau, Henning Voss
Johannes Kepler University Linz, Austria

Doctoral Program Computational Mathematics
Numerical Analysis and Symbolic Computation
FWF Der Wissenschaftsfonds.
JOHANNES KEPLER UNIVERSITY LINZ
LAND OBERÖSTERREICH

Introduction

The pulse wave velocity (PWV) in major arteries contains information about arterial compliance, which is an important determinant of the state of the cerebrovascular system. With respect to the brain, aortic stiffness, for example, has been associated with cerebral small-vessel disease in hypertensive patients and cognitive decline. By the Moens-Korteweg formula, the PWV is also connected to important physical parameters:

$$\text{PWV} = \sqrt{\frac{Eh}{\rho_B d}}\,, \qquad d \ldots \text{vascular diameter}\,, \quad h \ldots \text{vessel wall thickness}\,, \quad E \ldots \text{vessel wall's Young's modulus}\,, \quad \rho_B \ldots \text{density of blood}\,.$$

Magnetic Resonance Advection Imaging (MRAI)
In [1], Voss et al. introduced MRAI, a method to *estimate the PWV from dynamic MRI data*, based on an advection equation. We tried to improve their method by considering the underlying parameter estimation problem in the framework of Inverse Problems [2], leading to the algorithm presented here.

Mathematical Model and Discretization

If we denote by $v = v(x, y, z)$ the time-independent PWV vector field and with $\rho = \rho(x, y, z, t)$ the time-dependent dynamic MRI data, then a model connecting those two quantities is the advection equation:

$$\frac{\partial}{\partial t}\rho(x,y,z,t) + \nabla\rho(x,y,z,t)\cdot v(x,y,z) = 0\,, \quad (x,y,z)\in\Omega\,, t\in[0,T]\,. \tag{1}$$

To derive this equation, the additional assumption $\nabla \cdot v = 0$ is made and therefore must also be treated. Due to the measurement process (ascending slice acquisition), the data ρ is only given at the following points:

$$(x_i, y_j, z_k, t_{k,l})\,, \qquad 0 \le i \le I,\ 0 \le j \le J,\ 0 \le k \le K,\ 0 \le l \le L,$$
$$x_i := x_0 + i\Delta x\,, \quad y_j := y_0 + j\Delta y\,, \quad z_k := z_0 + k\Delta z\,, \quad t_{k,l} := (k + (K+1)l)\Delta t\,.$$

We now discretize (1) according to the data, which leads to

$$\frac{\rho_{i,j,k,l} - \rho_{i,j,k,l-1}}{(K+1)\Delta t} + D_{x_i}\rho_{i,j,k,l}\, v_{1,i,j,k} + D_{y_j}\rho_{i,j,k,l}\, v_{2,i,j,k} + D_{z_k}\rho_{i,j,k,l}\, v_{3,i,j,k} = 0\,, \tag{2}$$

where $\rho_{i,j,k,l} = \rho(x_i, y_j, z_k, t_{k,l})$ and $v_{s,i,j,k} = v_s(x_i, y_j, z_k)$ for $s = 1, 2, 3$. The operators D_{x_i}, D_{y_j} and D_{z_k} are finite difference approximations of the differential quotients w.r.t. x_i, y_j and z_k, respectively. In their definition, the limited amount of data due to the measurement process must be taken into account!

Collecting the $\rho_{i,j,k,l}$ values ($l > 0$) into a vector $\vec{\rho}$, the $\rho_{i,j,k,l}$ values ($l = 0$) into a vector $\vec{\rho}_0$ and the $v_{s,i,j,k}$ values into a vector $\vec{v}$, we can write (2) in the matrix-vector form

$$A(\vec{v})\vec{\rho} = b(\vec{v}, \vec{\rho}_0)\,. \tag{3}$$

The forward advection problem consists of calculating $\vec{\rho}$ from given $\vec{v}$ and $\vec{\rho}_0$ by solving the linear system (3).

The Inverse Problem

We consider the inverse problem of calculating $\vec{v}$ and $\vec{\rho}_0$ from given $\vec{\rho}$ data. Defining the nonlinear operator

$$F : \mathcal{X} \to \mathcal{Y}\,, \quad (\vec{v}, \vec{\rho}_0) \mapsto (\rho(\vec{v}, \vec{\rho}_0), \vec{\rho}_0, D\vec{v})\,,$$

where $\rho(\vec{v}, \vec{\rho}_0)$ denotes the solution of (3), $\mathcal{X}$ and $\mathcal{Y}$ are suitable vector spaces and D is matrix such that $D\vec{v}$ approximates the divergence of v, we arrive at the following inverse problem in standard form:

Inverse Problem of MRAI
Approximate $(\vec{v}, \vec{\rho}_0)$, which is the solution of the nonlinear equation

$$F(\vec{v}, \vec{\rho}_0) = (\vec{\rho}, \vec{\rho}_0, \vec{0})\,, \tag{4}$$

where, instead of $\vec{\rho}$ and $\vec{\rho}_0$, only noisy (measurement) data $\vec{\rho}^{\delta}$ and $\vec{\rho}_0^{\delta}$ are given.

The choice of the vector spaces $\mathcal{X}$ and $\mathcal{Y}$ and their inner products is of great importance. We use an inner product on $\mathcal{X}$ which leads to smooth velocity reconstructions and which is realized numerically using wavelets.

Reconstruction Algorithm

In order to obtain a stable approximation of the solution of the inverse problem (4), we minimize the functional

$$\frac{1}{2}\left\| F(\vec{v}, \vec{\rho}_0) - (\vec{\rho}^{\delta}, \vec{\rho}_0^{\delta}, 0)\right\|_{\mathcal{Y}}^2 + \alpha \left\|(\vec{v}, \vec{\rho}_0)\right\|_{\ell_1}\,,$$

using the following iterative algorithm (for readability, $x_k^{\delta} = (\vec{v}_k^{\delta}, \vec{\rho}_{0,k}^{\delta})$, $y^{\delta} = (\vec{\rho}^{\delta}, \vec{\rho}_0^{\delta}, 0)$):

$$z_k^{\delta} = x_k^{\delta} + \tfrac{k-1}{k+2}\left(x_k^{\delta} - x_{k-1}^{\delta}\right)\,, \quad \omega_k^{\delta} = \omega^{\delta}(z_k^{\delta})\,,$$
$$x_{k+1}^{\delta} = S_{\alpha\omega_k^{\delta}}\left(z_k^{\delta} + \omega_k^{\delta} F'(z_k^{\delta})^*(y^{\delta} - F(z_k^{\delta}))\right)\,,$$
$$x_0^{\delta} = x_{-1}^{\delta} = x_0\,,$$

where x_0 is an initial guess, $\omega^{\delta}(z_k^{\delta})$ is the *steepest descent* stepsize defined by

$$\omega^{\delta}(z) := \frac{\left\|s^{\delta}(z)\right\|^2}{\left\|F'(z)s^{\delta}(z)\right\|^2}\,, \qquad s^{\delta}(z) := F'(z)^*(y^{\delta} - F(z))\,,$$

and $S_{\alpha\omega_k^{\delta}}$ is a *shrinkage function*, which acts on a vector $\vec{w} = [\vec{w}_k]_{k\in\Lambda}$ via

$$S_{\alpha\omega_k^{\delta}}(\vec{w}) := [\text{sgn}(\vec{w}_k)\max(|\vec{w}_k| - \alpha\omega_k^{\delta}, 0)]_{k\in\Lambda}\,.$$

This method is based on the *iterative shrinkage thresholding algorithm*, the *steepest descent method* and *Nesterov's acceleration strategy*. In order to stop the iteration, we employ the well-known *discrepancy principle*.

Numerical Simulation

We first tested our algorithm on a 3D numerical simulation phantom featuring several vessels of different size, shape and orientation. Through each vessel, the initial signal

$$\rho_0(x,y,z) = \sin\left(\frac{6\pi}{\|\bar{v}\|_2}\left(\frac{\bar{v}_1}{I\Delta x}x + \frac{\bar{v}_2}{J\Delta y}y + \frac{\bar{v}_3}{K\Delta z}z\right)\right)$$

is transported via constant velocity vector fields $\bar{v} = (\bar{v}_1, \bar{v}_2, \bar{v}_3)$ and the data is created by using the fact that in this case the function

$$\rho(x,y,z,t) = \rho_0(x - \bar{v}_1 t, y - \bar{v}_2 t, z - \bar{v}_3 t)\,,$$

solves the advection equation (1). Afterwards, random noise of 1% magnitude has been added to the data. The figures below depict information about the real (upper two) and the reconstructed (lower two) velocity vector fields. The left figures show maximum intensity projections (MIPs) over the z-axis of the norm of the velocity fields and the right figures present colour direction MIPs, which depict the direction in which the velocity fields are pointing (red = x-axis, green = y-axis, blue = z-axis).

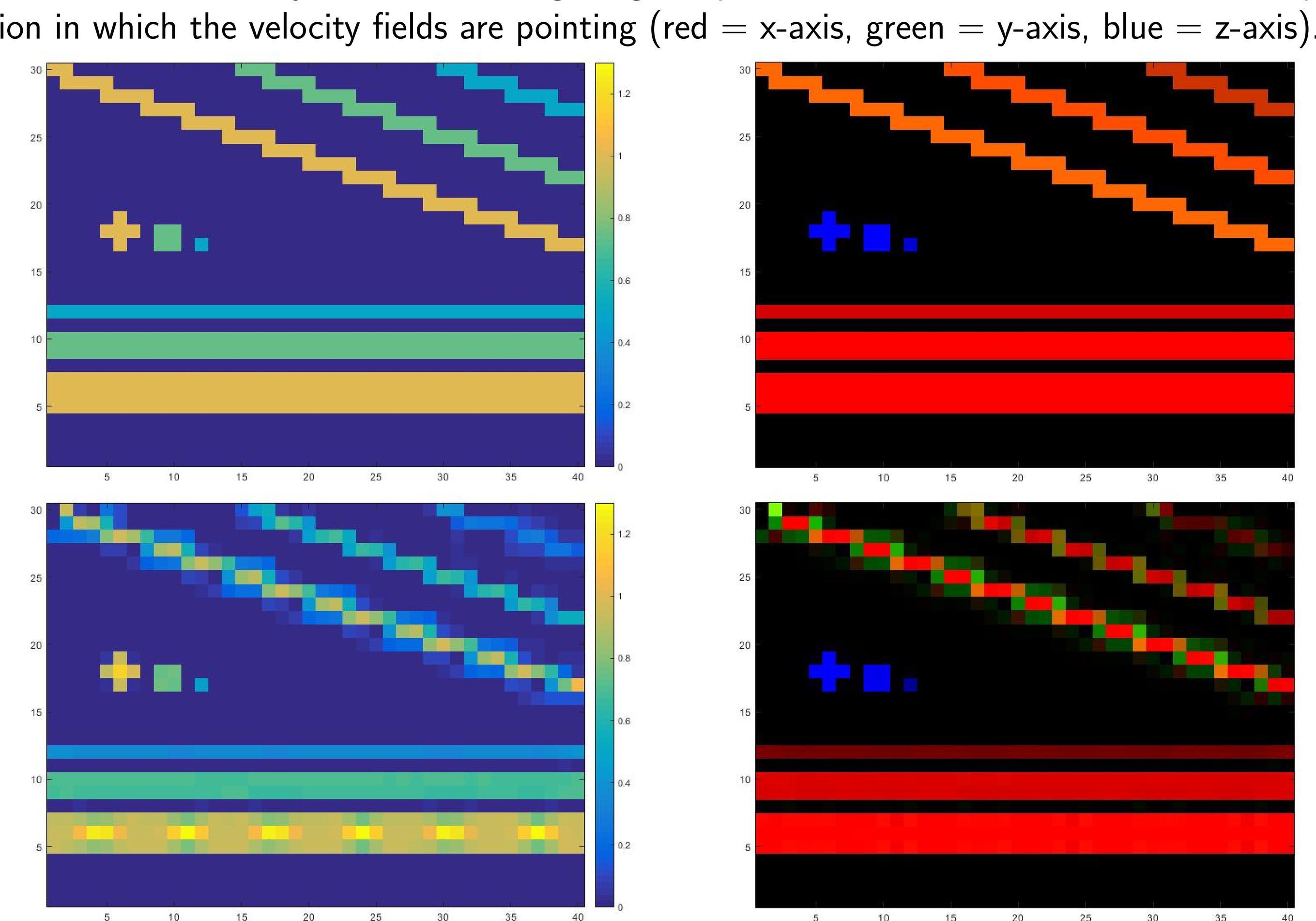

Real-World Data Set

The figures below again show a MIP and a colour direction MIP, this time of the results of our algorithm applied to subject 16 of a publicly available natural stimulation dynamic EPI data set obtained on a 7.0 T MRI scanner [3]. The first $20\,$s of the second measurement segment were used. The transversal slices covered most of the frontal and occipital cortex and the regions in between. The data was sampled with a pulse repetition time of $2\,$s and an isotropic spatial resolution of $1.4\,$mm.

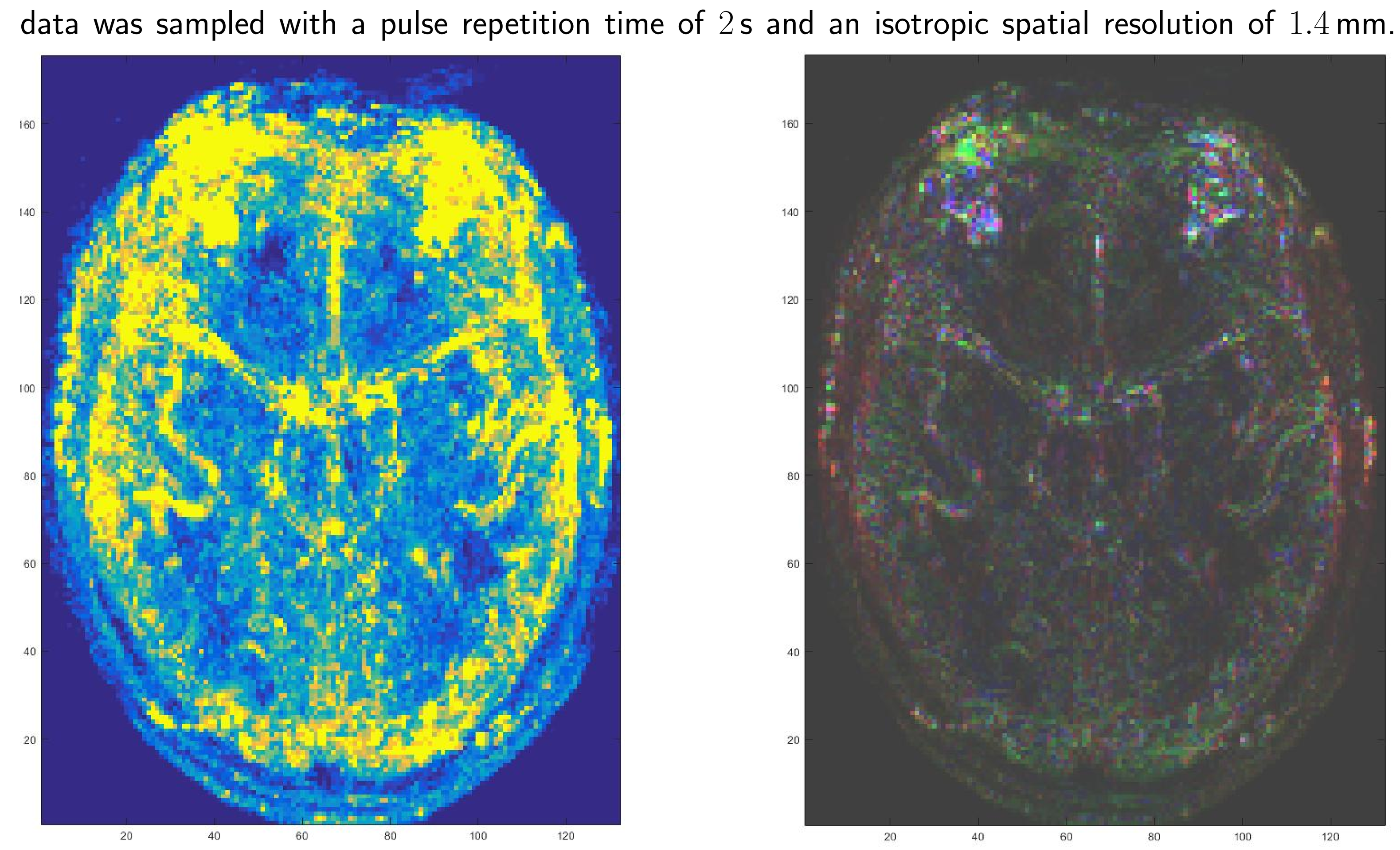

The location of the major blood vessels and arteries, as well as the orientation of the PWV vector field, are clearly visible. However, due to the rather low (spatio)temporal resolution, only qualitative information about the PWV can be obtained at the moment. One possible way towards quantitative results would be the use of more advanced imaging methods such as multiband EPI, which could potentially yield data sets with the required resolution.

References

[1] H. U. Voss, J. P. Dyke, K. Tabelow, N. D. Schiff, and D. J. Ballon. Magnetic resonance advection imaging (MRAI) of cerebrovascular pulse dynamics. *JCBFM*, in press.

[2] S. Hubmer, A. Neubauer, R. Ramlau, and H. U. Voss. On the Parameter Estimation Problem of Magnetic Resonance Advection Imaging. In preparation.

[3] M. Hanke, F. J. Baumgartner, P. Ibe, F. R. Kaule, S. Pollmann, O. Speck, W. Zinke, and J. Stadler. A high-resolution 7-Tesla fMRI dataset from complex natural stimulation with an audio movie. *Sci Data*, 1:140003:1–18, 2014.